Biomedical Research and Therapy 2026, 13(08):8853-8868

Open Access Full Text Article

Original Research

Structure-Based Identification of Multi-Target Phytochemical Inhibitors from *Garuga pinnata* and *Mitragyna speciosa* Targeting the AXL Kinase and TGF-β Receptor Axis: An *In Silico* Study

Mohammad Nadeem Khan[1,*], Mahak Bhandari[2], Ashok Kumar[3], Praveen Chandra Dubey[4], Sanjay Vyas[5], Shushil Upadhayay[6]

ABSTRACT

Background: Metastasis is the primary cause of cancer-related mortality and is driven by dysregulated signaling pathways, including AXL kinase and the transforming growth factor-beta (TGF-β) receptor axis. Targeting these interconnected pathways represents a promising strategy to suppress epithelial–mesenchymal transition (EMT) and metastatic progression. **Methods:** This study employed an integrated *in silico* approach to evaluate phytochemicals from *Garuga pinnata* and *Mitragyna speciosa* as potential multi-target ligands. Molecular docking was performed using CB-Dock, followed by interaction analysis with Discovery Studio Visualizer. Binding free energy estimation was conducted using MM/GBSA and MM/PBSA methods, and structural consistency of docked complexes was assessed using RMSD analysis. Four receptors—AXL kinase (5U6B), TGF-β1 (3KFD), TGF-βRII (3DKC), and TGF-βRI kinase (3ODU)—were selected for evaluation. **Results:** Selected phytochemicals, including 7-acetoxymitragynine, mitraphylline-26, and 21-hydroxydammar-24-en-3-one, exhibited favorable binding affinities (ΔG ≈ −16 to −14 kcal/mol) across multiple targets. Interaction analysis revealed consistent hydrogen bonding patterns, hydrophobic contacts, and π-mediated interactions with key residues such as Asp70, Glu74, Arg163, and Tyr185. RMSD values (< 2.5 Å) indicated consistent binding orientations within receptor pockets, supporting structural compatibility. **Conclusion:** The findings demonstrated a scaffold-dependent, multi-target binding profile of phytochemicals against the AXL–TGF-β signaling axis. While the results provided a computational basis for prioritizing candidate ligands, further validation through molecular dynamics simulations and experimental studies is required to confirm their therapeutic potential in anti-metastatic drug discovery.

Key words: AXL kinase, TGF-β receptor, Molecular docking, *Mitragyna speciosa*, *Garuga pinnata*

[1]*Department of Pharmacology (Clinical Pharmacology), Sri Aurobindo Medical College & PG Institute, Sri Aurobindo University Indore, Madhya Pradesh, India-453555*

[2]*Department of Surgery, Sri Aurobindo Medical College & PG Institute, Sri Aurobindo University Indore, Madhya Pradesh, India-453555*

[3]*Department of Pharmacology, Sri Aurobindo Medical College & PG Institute, Sri Aurobindo University Indore, Madhya Pradesh, India-453555*

[4]*Department of Botany, Devi Ahilya Vishwavidyalaya, Indore (M.P.), India-452001*

[5]*Department of Microbiology and Horticulture, Government Holkar Science College, Indore, India,452002*

[6]*Sri Aurobindo University, Indore, Madhya Pradesh, India*

Correspondence

Mohammad Nadeem Khan ,
Department of Clinical Pharmacology, Sri Aurobindo Medical College & PG Institute, Indore, Madhya Pradesh, India

Email:
sahani.nadeem35@gmail.com

INTRODUCTION

Metastasis remains the leading cause of cancer-related mortality, contributing to nearly 90% of cancer-associated deaths worldwide [1]. This multistep process is governed by a complex interplay of oncogenic signaling pathways, epithelial–mesenchymal transition (EMT), extracellular matrix remodeling, and immune evasion mechanisms that collectively enable tumor dissemination and colonization of distant organs [2]. Among these regulatory networks, the receptor tyrosine kinase AXL and the transforming growth factor-beta (TGF-β) signaling axis have emerged as critical mediators of tumor progression, therapeutic resistance, and adverse clinical outcomes [3,4]. Their coordinated activation promotes EMT, enhances cellular plasticity, and facilitates immune suppression, positioning them as strategically important yet underexploited targets in anti-metastatic intervention [5].

The AXL receptor tyrosine kinase (PDB ID: 5U6B), a member of the TAM (TYRO3–AXL–MERTK) family, plays a pivotal role in regulating cell survival, migration, and invasion through activation of downstream pathways such as PI3K/Akt, MAPK, and NF-κB [6]. Aberrant overexpression of AXL has been documented across multiple malignancies, including breast, lung, pancreatic, and hepatocellular cancers, where it correlates strongly with metastatic potential and resistance to conventional therapies [7]. In parallel, the TGF-β signaling pathway—mediated by TGF-β1 (3KFD) and its receptors TGF-βRII (3DKC) and TGF-βRI kinase (3ODU)—exhibits a context-dependent dual role in oncogenesis, functioning as a tumor suppressor in the early stages while promoting EMT, stromal remodeling, and immune eva-

Cite this article : Khan MN, Bhandari M, Kumar A, Dubey PC, Vyas S, Upadhayay S. **Structure-Based Identification of Multi-Target Phytochemical Inhibitors from *Garuga pinnata* and *Mitragyna speciosa* Targeting the AXL Kinase and TGF-β Receptor Axis: An *In Silico* Study**. *Biomed. Res. Ther.* 2026; 13(08):8853-8868.

History
- Received: Nov 20, 2025
- Accepted: Jul 06, 2026
- Published Online: Aug 31, 2026

DOI : 10.15419/bmrat.v13i8.1091

sion during advanced disease progression [8,9]. Importantly, emerging evidence suggests that crosstalk between the AXL and TGF-β signaling pathways synergistically amplifies EMT and metastatic dissemination, thereby providing a compelling rationale for their dual targeting [10].

Despite their biological significance, currently available inhibitors targeting AXL and TGF-β receptors are limited by issues such as suboptimal selectivity, off-target toxicity, and restricted clinical efficacy [11]. These challenges underscore the need for alternative therapeutic strategies, particularly those capable of modulating multiple signaling nodes simultaneously. In this context, phytochemical-based therapeutics have gained increasing attention due to their structural diversity, pharmacological versatility, and generally favorable safety profiles [12]. Natural compounds derived from ethnomedicinal plants represent a valuable and sustainable reservoir for the discovery of multi-target bioactive molecules, especially in complex diseases such as cancer where network-level modulation is required [13].

In this study, we explored a structure-based computational framework to identify potential multi-target phytochemical modulators from *Garuga pinnata* and *Mitragyna speciosa*, two ethnopharmacologically significant species with documented anti-inflammatory and anticancer properties [14]. Although these plants are rich in bioactive alkaloids, flavonoids, and terpenoids, their mechanistic roles in modulating metastasis-associated signaling pathways remain insufficiently characterized.

MATERIALS & METHODS

Selection of Ethnomedicinal Plants and Phytochemicals

Garuga pinnata and *Mitragyna speciosa* were selected based on their well-documented ethnomedicinal use among tribal populations of the Narmada Valley region (Alirajpur, Jhabua, and Dhar, Madhya Pradesh, India), where they are traditionally employed in the management of inflammation, pain, and fatigue-associated conditions [15]. Ethnopharmacological knowledge provides a biologically relevant framework for identifying candidate molecules with potential activity against complex, multi-pathway diseases such as cancer [16]. A systematic phytochemical profiling approach was performed using curated chemical databases, including PubChem, IMPPAT, and ChEMBL [17]. Compounds were prioritized based on reported pharmacological relevance, structural diversity, and the availability of validated chemical structures. A total of fifteen phytochemicals was selected, comprising seven compounds from *G. pinnata* and eight from *M. speciosa*. These compounds represented distinct chemical classes, including diterpenoids and indole alkaloids, which are known for their diverse pharmacological activities. A summary of the selected compounds, their classification, and selection rationale is presented in Table 1.

All ligand structures were retrieved in SDF format and subjected to geometry optimization using Open Babel (v2.4.1) to obtain energetically stable conformations prior to docking [18]. The optimized structures were converted into PDBQT format to ensure compatibility with docking algorithms. Drug-likeness evaluation was performed according to Lipinski's Rule of Five, assessing molecular weight, lipophilicity (logP), hydrogen bond donors and acceptors, and rotatable bond count [19]. This screening ensured that the selected phytochemicals possessed favorable physicochemical properties consistent with oral bioavailability and pharmacokinetic suitability.

Receptor Selection and Preparation

Four metastasis-associated protein targets were strategically selected based on their well-established roles in regulating epithelial–mesenchymal transition (EMT), tumor invasiveness, and metastatic progression: AXL kinase (PDB ID: 5U6B), TGF-β1 (PDB ID: 3KFD), TGF-β receptor II (PDB ID: 3DKC), and TGF-β receptor I kinase (PDB ID: 3ODU) [20]. The three-dimensional structures of these receptor proteins are illustrated in Figure 1. The simultaneous targeting of these receptors enabled the exploration of a multi-pathway inhibition strategy within the AXL–TGF-β signaling axis, which is known to synergistically drive metastatic phenotypes. Three-dimensional crystal structures were retrieved from the Protein Data Bank (PDB) and subjected to standardized preprocessing to ensure structural reliability for docking simulations. This included the removal of crystallographic water molecules, heteroatoms, and co-crystallized ligands to eliminate potential steric and electrostatic interference [21]. Polar hydrogen atoms were subsequently added, and structural optimization was performed using Discovery Studio Visualizer to stabilize protein geometry and prepare the receptors for interaction analysis. Binding pocket identification was performed using complementary computational tools, including CASTp and CB-Dock, allowing accurate detection

Table 1: Summary of Selected Phytochemicals and Key Properties

Plant Source	Compound Class	No. of Compounds	Representative Molecules	Selection Rationale
Garuga pinnata	Diterpenoids	7	21-hydroxydammar-24-en-3-one, Garuganin-V derivatives	Large scaffolds suitable for kinase binding
Mitragyna speciosa	Indole alkaloids	8	7-acetoxymitragynine, Mitraphylline-26	Aromatic structures enabling π–π interactions

of ligand-accessible cavities based on geometric and topological features[22]. The identified binding sites exhibited significant variability in pocket volume and residue composition, ranging from 630 $Å^3$ (TGF-βRII) to 3503 $Å^3$ (TGF-β1), highlighting differences in ligand accommodation capacity and physicochemical environments across targets. A comparative summary of receptor characteristics, including structural properties and binding pocket features, is presented in Table 2, providing a foundation for understanding differential ligand binding behavior across the selected targets.

Molecular Docking and Binding Site Validation

Molecular docking was performed using CB-Dock (v2.0), which integrates cavity detection with Auto_Dock Vina scoring to predict ligand-binding conformations[23]. A blind docking approach was employed to identify both canonical and potential allosteric binding sites without predefined bias. The docking search space for each receptor was defined based on the top-ranked predicted cavities, and detailed grid parameters including center coordinates and box dimensions were provided in Table 3 to ensure reproducibility. Binding affinities were expressed as estimated Gibbs free energy (ΔG, kcal/mol), where more negative values indicated stronger predicted interactions. Post-docking interaction profiling, including hydrogen bonding, hydrophobic contacts, and π-mediated interactions, was performed using Discovery Studio. Ligand efficiency was calculated to normalize binding affinity relative to molecular size.

Docking Protocol Validation

Given the blind docking framework employed by CB-Dock, conventional validation through redocking of co-crystallized ligands was not uniformly feasible across all receptor systems. To address this limitation, a residue-based validation strategy was implemented, wherein predicted ligand-binding poses were evaluated against literature-reported active site residues of AXL kinase and TGF-β receptors[24–26]. The consistent involvement of key residues—such as Asp70, Glu74, Arg163, and Tyr185—supports the biological relevance and structural plausibility of the predicted binding modes. Furthermore, docking poses and interaction geometries were independently examined using Discovery Studio Visualizer to verify hydrogen bonding patterns, steric compatibility, and overall binding orientation within the receptor cavities. The observed interaction profiles, including hydrogen bonding and π-mediated contacts within known functional domains, were consistent with established ligand–receptor interaction principles. Although this approach provided indirect validation, it is consistent with accepted practices in blind docking workflows where experimentally resolved reference ligands are unavailable[27]. Nevertheless, it is acknowledged that docking predictions represent static approximations; therefore, future studies will incorporate re-docking protocols, consensus docking approaches, and molecular dynamics simulations to enhance predictive reliability and dynamic accuracy.

Binding Free Energy Estimation (MM/GBSA and MM/PBSA)

To complement docking-based affinity predictions, binding free energy calculations were performed using MM/GBSA and MM/PBSA approaches, which integrate molecular mechanics energy terms with implicit solvation models to evaluate ligand–receptor interaction energetics[28]. These methods were applied to comparatively assess binding favorability and to identify key residue-level energetic contributions involved in stabilizing the docked complexes.

The calculated free energy profiles generally supported the molecular docking results, in which top-ranked phytochemicals demonstrated favorable energetic stabilization within the receptor binding pockets. However, it is important to emphasize that these calculations were performed on energy-minimized static receptor–ligand complexes rather than on conformational ensembles generated

Table 2: Structural and Functional Characteristics of Selected Target Receptors

Receptor	PDB ID	Biological Role	Pocket Volume (Å^3)	Key Structural Features	Functional Relevance
AXL Kinase	5U6B	EMT, invasion, survival signaling	2048	ATP-binding cleft; acidic & aromatic residues	Regulates migration and drug resistance
TGF-β1	3KFD	EMT induction, immune modulation	3503	Large aromatic-rich cavity	Promotes metastasis in advanced cancer
TGF-βRII	3DKC	Signal transduction initiation	630	Compact amphipathic pocket	Controls ligand-mediated signaling
TGF-βRI Kinase	3ODU	SMAD activation, EMT signaling	2486	Balanced donor–acceptor residues	Drives downstream transcriptional responses

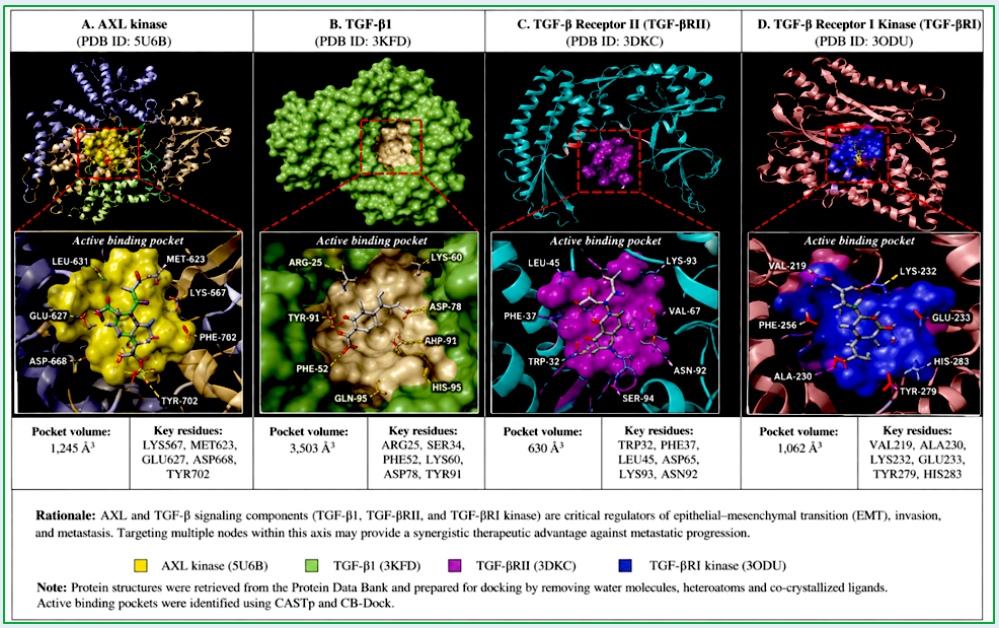

Figure 1: Structural overview of the metastasis-associated protein targets and their active ligand-binding pockets. Representative three-dimensional structures of AXL kinase (5U6B), TGF-β1 (3KFD), TGF-β receptor II (3DKC), and TGF-β receptor I kinase (3ODU) are shown with enlarged views of the predicted active binding pockets used for molecular docking and receptor–ligand interaction analyses. Protein structures were retrieved from the Protein Data Bank and binding sites were identified using CASTp and CB-Dock.

through molecular dynamics simulations. Therefore, the obtained ΔG values should be interpreted as relative and comparative estimates of binding favorability rather than absolute thermodynamic parameters.

In addition, the present approach did not account for time-dependent conformational flexibility, explicit solvent dynamics, or entropic contributions, all of which can influence the accuracy of free energy estimation under physiological conditions[29]. Accordingly, the MM/GBSA and MM/PBSA analyses in this study were used to support docking-derived interaction trends and to prioritize structurally compatible phytochemicals for further investigation, rather than to infer definitive binding stability. Future studies incorporating trajectory-based molecular dynamics simulations and advanced free energy calculations will be necessary to provide deeper insight into kinetic stability and thermo-

Table 3: Docking Parameters and Search Space Configuration

Receptor	PDB ID	Binding Site Type	Grid Box Size (Å)	Grid Center Coordinates (x, y, z)	Exhaustiveness	No. of Binding Modes	Key Functional Region
AXL Kinase	5U6B	ATP-binding cleft	25 × 25 × 25	Defined by CB-Dock predicted cavity center	12	9	Catalytic kinase domain
TGF-β1	3KFD	Ligand-binding interface	30 × 30 × 30	Defined by CB-Dock predicted cavity center	12	9	Cytokine interaction region
TGF-βRII	3DKC	Receptor binding pocket	22 × 22 × 22	Defined by CB-Dock predicted cavity center	12	9	Signal initiation domain
TGF-βRI Kinase	3ODL	Kinase active site	26 × 26 × 26	Defined by CB-Dock predicted cavity center	12	9	SMAD phosphorylation domain

(Docking cavities and corresponding grid center coordinates were automatically predicted using the CB-Dock v2.0 blind docking platform based on receptor surface topology and cavity detection algorithms.)

dynamic behavior of the identified ligand–receptor complexes.

Conformational Assessment (RMSD Analysis)

Root Mean Square Deviation (RMSD) analysis was performed using Discovery Studio to evaluate the structural consistency and conformational deviation of receptor–ligand complexes following energy minimization. RMSD values below 2.5 Å were considered indicative of limited structural fluctuation and consistent ligand accommodation within the predicted binding pockets. The analysis was used to assess the reliability of docking-derived binding geometries and overall pose consistency across receptor systems. However, it is important to note that these RMSD measurements were derived from static, energy-minimized complexes and therefore reflect structural consistency rather than time-dependent dynamic stability under physiological conditions[30].

Visualization and Interaction Mapping

Receptor–ligand complexes were visualized using Discovery Studio Visualizer. Two-dimensional and three-dimensional interaction maps were generated to illustrate hydrogen bonds, hydrophobic interactions, and electrostatic contacts within the binding pockets. Structural visualization facilitated the identification of key residues involved in ligand stabilization and provided insights into binding orientation and interaction networks[31].

Computational Workflow

The computational framework employed in this study comprised a structured, multi-step pipeline integrating receptor selection, ligand preparation, blind molecular docking, interaction profiling, binding free energy estimation, and structural deviation analysis (Figure 2, 3). Ethnomedicinally relevant phytochemicals were initially identified and prepared through energy minimization and format conversion, while target receptor structures were retrieved and processed to ensure suitability for docking simulations.

Binding pockets were identified using cavity detection tools, followed by blind docking to explore ligand–receptor interactions across multiple potential binding sites. Post-docking analyses included interaction mapping to characterize hydrogen bonding, hydrophobic contacts, and π-mediated interactions. Binding free energy estimation using MM/GBSA and MM/PBSA methods was performed to evaluate relative interaction favorability. Structural analysis using RMSD was conducted to assess conformational deviation of the docked complexes. This workflow enabled the systematic evaluation of ligand–receptor interactions and facilitated the identification of phytochemicals with potential multi-target binding affinity toward components of the AXL–TGF-β signaling axis.

RESULTS

Receptor Structural Characterization and Binding Pocket Topology

Structural characterization of the selected metastasis-associated receptors revealed distinct

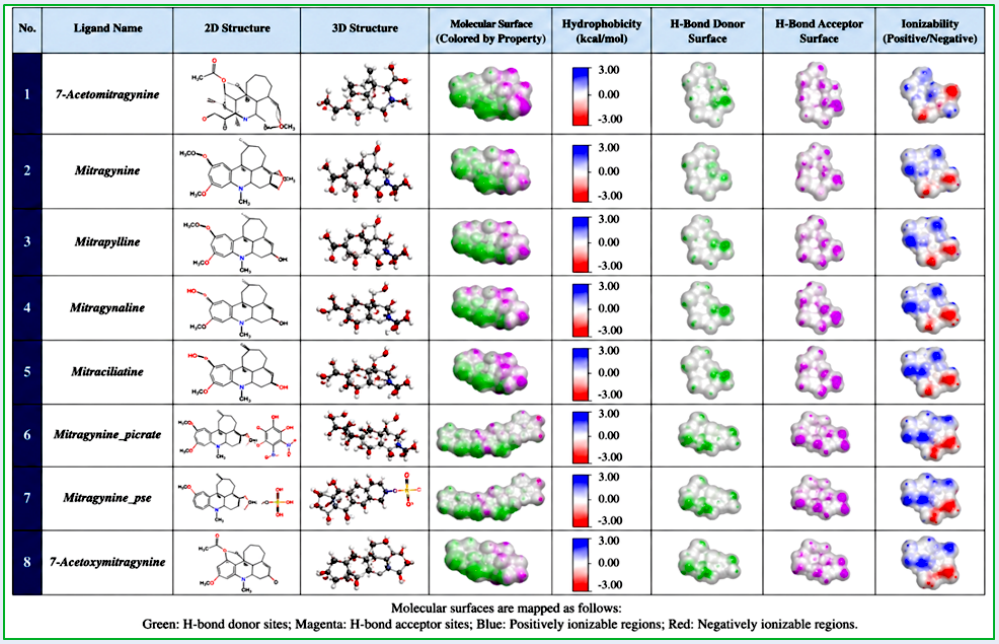

Figure 2: Comprehensive physicochemical profiling of selected *Mitragyna speciosa* phytochemicals. Representative 2D and 3D structures together with molecular surface properties, including hydrophobicity, hydrogen-bond donor/acceptor regions, and ionizable surfaces, illustrating the structural features that may influence receptor recognition and molecular docking performance.

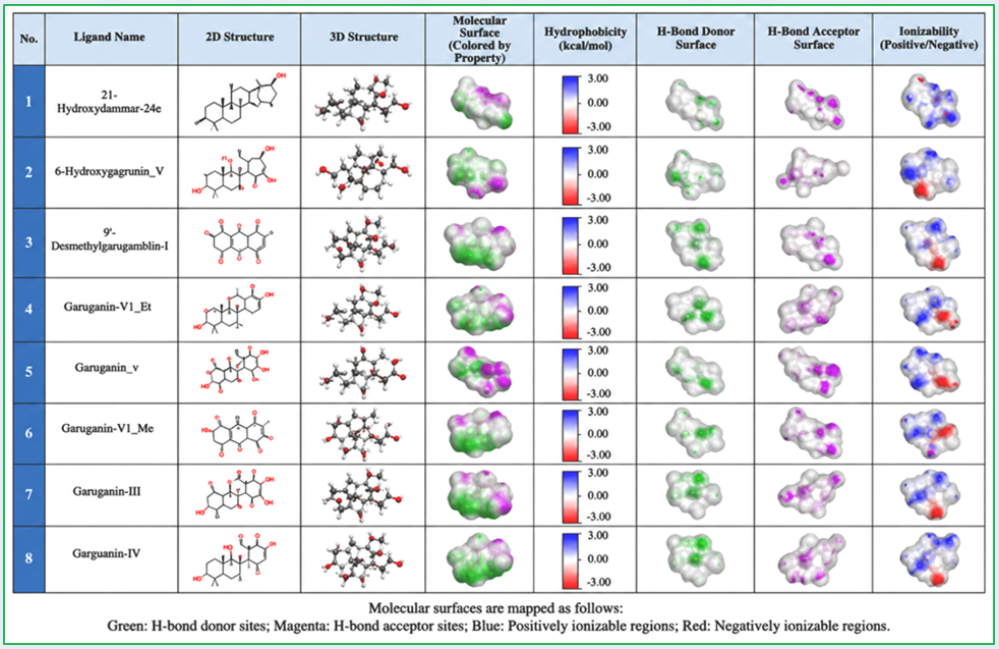

Figure 3: Comprehensive physicochemical profiling of selected *Garuga pinnata* phytochemicals. Representative 2D and 3D molecular structures together with molecular surface properties, including hydrophobicity, hydrogen-bond donor and acceptor regions, and ionizable surfaces, illustrating the structural features that influence ligand–receptor recognition and docking performance.

variations in binding pocket architecture, residue composition, and physicochemical properties that influenced ligand accommodation and interaction behavior (Table 4). Pocket volumes ranged from 630 Å^3 (TGF-βRII) to 3503 Å^3 (TGF-β1), indicating substantial variability in cavity size and flexibility. The AXL kinase domain (5U6B) exhibited a well-defined ATP-binding cleft enriched with acidic residues (Asp70, Glu74, Asp179) and aromatic residues (Phe36, Tyr187), forming a favorable electrostatic and hydrophobic environment for ligand binding. In contrast, TGF-β1 presented the largest and most aromatic-rich cavity, characterized by residues such as Trp30, Phe54, and Tyr69, supporting π–π interactions and preferential binding of aromatic ligands. TGF-βRII displayed a comparatively compact, amphipathic pocket dominated by Asp119, Arg163, and Tyr185, suggesting selective ligand accommodation. Meanwhile, TGF-βRI kinase exhibited a balanced donor–acceptor distribution (Arg80, Asp84, Tyr401), supporting stable ligand anchoring within its catalytic domain.

Overall, the presence of conserved acidic, basic, and aromatic residues across all receptors established a structurally compatible framework for multi-target ligand binding within the AXL–TGF-β signaling axis.

Molecular Docking and Binding Affinity Analysis

Molecular docking analysis demonstrated that phytochemicals derived from both *Garuga pinnata* and *Mitragyna speciosa* exhibited favorable binding affinities across all selected receptors, with clear differences observed based on ligand class and receptor topology (Table 5). Among *Garuga pinnata* compounds, 21-hydroxydammar-24-en-3-one showed consistently strong binding across multiple targets, with the highest affinity observed against TGF-βRII (ΔG = −16.8 kcal/mol) and AXL kinase (ΔG = −16.3 kcal/mol). Other diterpenoids, including Garuganin-V1_Et and Garuganin-V1_Me, also demonstrated favorable binding (ΔG ≈ −14.5 to −13.5 kcal/mol), indicating broad receptor compatibility. For *Mitragyna speciosa*, alkaloid derivatives such as 7-acetoxymitragynine and mitraphylline-26 exhibited strong binding interactions, particularly against AXL kinase (ΔG = −12.7 kcal/mol) and TGF-βRII (ΔG = −14.6 kcal/mol). These compounds showed consistent affinity across kinase and receptor targets, suggesting potential multi-target engagement. RMSD values for most ligand–receptor complexes remained within a low deviation range, indicating stable docking conformations and minimal structural perturbation within the predicted binding pockets.

Interaction Mapping and Residue-Level Binding Analysis

Post-docking visualization of the receptor–ligand complexes (Figures 4 and 5) revealed that the selected phytochemicals adopted well-defined orientations within the binding pockets of AXL kinase and TGF-β receptors, demonstrating consistent spatial accommodation and alignment with key functional regions. In AXL kinase, ligands were predominantly positioned within the ATP-binding cleft, exhibiting a stable orientation along the catalytic groove, where their hydrophobic cores aligned with aromatic residues while polar functional groups extended toward solvent-accessible regions, facilitating hydrogen bonding. Similarly, in TGF-β receptors, ligands occupied central cavity regions with orientations that maximized surface complementarity, allowing simultaneous engagement of polar and hydrophobic residues within the pocket. The visual representations further indicated that high-affinity phytochemicals maintained compact and well-fitted conformations, with minimal steric clashes and favorable pocket occupancy. Diterpenoid scaffolds tended to occupy deeper regions of larger cavities, whereas indole alkaloids aligned along aromatic-rich surfaces, supporting π-mediated interactions. Overall, the observed ligand orientations and binding site conformations demanded (or demonstrated) a high degree of geometric compatibility between phytochemicals and receptor pockets, reinforcing their ability to effectively engage multiple targets within the AXL–TGF-β signaling axis.

Binding Free Energy Analysis (MM/GBSA and MM/PBSA)

Binding free energy calculations using MM/GBSA and MM/PBSA were performed to refine docking-based rankings and to quantify residue-level contributions to ligand stabilization (Table 6). Across targets, the calculated ΔG values were consistently negative, indicating energetically favorable ligand–receptor associations and supporting the trends observed in molecular docking. Among *Mitragyna speciosa* alkaloids, 7-acetoxymitragynine exhibited the most favorable binding against AXL kinase (ΔG ≈ −45.2 kcal/mol), characterized by a combination of hydrogen bonding and electrostatic interactions within the catalytic domain. Mitraphylline-26 also

Table 4: Structural Topology and Binding Pocket Characteristics of Target Receptors Relevant to Ligand Accommodation

Receptor (PDB ID)	Pocket Volume (Å^3)	Pocket Nature	Key Donor Residues	Key Acceptor Residues	Aromatic / Hydrophobic Residues	Structural Interpretation	Docking Relevance
AXL Kinase (5U6B)	2048	Moderately large, catalytic cleft	Lys56, Ser73, Thr64	Asp70, Glu74, Asp179	Phe36, Leu182, Met58, Tyr187	ATP-binding pocket with strong electrostatic gradient and aromatic stabilization	Favors bulky hydrophobic ligands with π-interaction capability
TGF-β1 (3KFD)	3503	Large, aromatic-rich cavity	Lys31, Arg52, Ser60	Asp104, Glu99	Trp30, Trp32, Phe54, Tyr69	Highly flexible cavity enriched with π-active residues	Suitable for aromatic alkaloids enabling π–π stacking interactions
TGF-βRII (3DKC)	630	Compact, amphipathic pocket	Arg163, Lys187	Asp119, Asp177	Tyr185, Met166	Small, selective binding pocket with mixed polarity	Prefers compact ligands with balanced polarity and size
TGF-βRI Kinase (3ODU)	2486	Deep kinase domain cavity	Arg80, Lys410	Asp84, Glu288	Tyr401, Phe423, Tyr476	Balanced donor–acceptor and hydrophobic environment	Supports stable ligand anchoring and multi-point interactions

demonstrated strong stabilization, primarily driven by cation–π and electrostatic contributions within receptor cavities. For *Garuga pinnata*, diterpenoid scaffolds showed consistent energetic stabilization across receptors, with key contributions from hydrogen bonding and hydrophobic interactions involving residues such as Asp161, Asp179, and Phe36 within the kinase-associated regions. Importantly, these energy estimates were derived from energy-minimized static complexes and therefore represented relative binding favorability rather than absolute thermodynamic parameters. Within this context, the MM/GBSA and MM/PBSA results served to corroborate docking-derived trends and supported the prioritization of phytochemicals exhibiting stable and energetically favorable interaction profiles.

Structural Consistency Assessment

Structural consistency of the top-ranked phytochemical–receptor complexes was evaluated using RMSD analysis derived from docking-based energy-minimized structures. As summarized in Table 7 and illustrated in Figure 6, most ligand–receptor complexes exhibited low RMSD values, generally below 3.0 Å, indicating limited conformational deviation and consistent ligand accommodation within the predicted receptor binding pockets. These findings supported the structural reliability of the docking-derived binding geometries and suggested favorable spatial orientation of the phytochemicals within metastasis-associated receptor cavities.

Among the evaluated compounds, 21-hydroxydammar-24-en-3-one from *Garuga pinnata* demonstrated the lowest RMSD value against TGF-βRII (3DKC) (0.586 Å), reflecting highly consistent pocket accommodation and favorable structural stabilization within the compact receptor cavity (Table 7; Figure 5, 6). Similarly, the indole alkaloids 7-acetoxymitragynine and 7-hydroxymitragynine from *Mitragyna speciosa* exhibited low RMSD values against AXL kinase (5U6B), supporting favorable ligand orientation and structurally coherent interaction geometry within the catalytic region. Other phytochemicals, including Garuganin-V1_Et, Garuganin-V1_Me, and Mitraphylline-26, also maintained relatively low conformational deviation, suggesting consistent docking conformations across multiple receptor environments. Comparative RMSD analysis further

Table 5: Integrated Comparative Molecular Docking and Stability Profile of Phytochemicals from *Garuga pinnata* and *Mitragyna speciosa*

Ligand	Source	Chemical Class	Best Target Receptor	Binding Affinity (ΔG, kcal/mol)	Structural Interpretation	Multi-Target Potential
21-Hydroxydammar-24-en-3-one	*Garuga pinnata*	Diterpenoid	TGF-βRII (3DKC)	−16.8	Bulky hydrophobic scaffold fits deep catalytic pocket with strong van der Waals stabilization	High
Garuganin-V1_Et	*Garuga pinnata*	Diterpenoid	TGF-βRII	−14.5	Flexible side chains enhance conformational adaptability	High
Garuganin-V1_Me	*Garuga pinnata*	Diterpenoid	TGF-βRII	−13.8	Compact derivative supports stable binding geometry	High
6-Hydroxygaruganin-V	*Garuga pinnata*	Diterpenoid	AXL kinase (5U6B)	−13.6	Balanced polarity enables hydrogen bonding and electrostatic interactions	Moderate–High
7-Acetoxymitragynine	*Mitragyna speciosa*	Indole Alkaloid	TGF-βRII	−14.6	Aromatic scaffold supports π–π and cation–π interactions	High
Mitraphylline-26	*Mitragyna speciosa*	Indole Alkaloid	TGF-βRII	−13.1	Rigid structure ensures stable orientation in pocket	High
7-Hydroxymitragynine	*Mitragyna speciosa*	Indole Alkaloid	AXL kinase	−11.9	Highly stable conformation with minimal structural deviation	High
Mitragynine	*Mitragyna speciosa*	Indole Alkaloid	Multiple	−8.9 to −9.3	Moderate polarity limits deep pocket interaction	Moderate
Mitragynaline / Mitraciliatine	*Mitragyna speciosa*	Indole Alkaloid	Multiple	−8.4 to −9.4	Reduced aromatic interaction limits stabilization	Moderate
Garuganin-III / IV / Desmethyl derivatives	*Garuga pinnata*	Diterpenoid	Multiple	−6.7 to −9.1	Lower hydrophobic surface reduces binding strength	Moderate

indicated scaffold-dependent accommodation patterns, in which diterpenoid compounds preferentially aligned within deeper hydrophobic cavities, while indole alkaloids demonstrated effective adaptation within aromatic-rich binding regions, as represented in Figure 5, 6.

Importantly, the structural consistency observed through RMSD evaluation correlated well with the molecular docking, interaction mapping, and MM/GBSA–MM/PBSA analyses, collectively supporting the structural compatibility of these phytochemicals with key components of the AXL–TGF-β signaling axis. Within the limitations of a static computational framework, these findings provided additional structural validation for the predicted ligand–receptor interactions and supported the prioritization of selected ethnopharmacological scaffolds for future experimental investigation.

Integrated Multi-Target Binding Perspective

Collectively, the integrated computational analyses demonstrated that phytochemicals derived from *Garuga pinnata* and *Mitragyna speciosa* exhibited consistent binding trends, favorable interaction profiles, and structurally coherent docking conforma-

Table 6: MM/GBSA and MM/PBSA Binding Free Energy Profile of Selected Phytochemical–Receptor Complexes

Ligand	Source	Target Receptor	MM/GBSA ΔG (kcal/mol)	MM/PBSA ΔG (kcal/mol)	Dominant Interaction Type	Key Residues Involved	Energetic Interpretation
21-Hydroxy-dammar-24-en-3-one	*Garuga pinnata*	TGF-βRII	−36.8	−34.5	Hydrophobic + H-bond	Asp119, Tyr185	Deep pocket accommodation with hydrophobic stabilization
Garuganin-V1_Et	*Garuga pinnata*	TGF-βRI (3ODU)	−34.2	−32.7	Hydrophobic + Electrostatic	Glu288, Tyr401	Flexible scaffold enables multi-point interaction
Garuganin-V1_Me	*Garuga pinnata*	AXL Kinase	−32.5	−30.8	Hydrophobic	Phe36, Met58	Moderate stabilization via non-polar interactions
7-Acetoxymitragynine	*Mitragyna speciosa*	AXL Kinase (5U6B)	−45.2	−42.8	H-bond + Electrostatic	Asp70, Glu74, Asp179	Highly favorable stabilization with strong electrostatic contribution
Mitraphylline-26	*Mitragyna speciosa*	TGF-βRII (3DKC)	−41.6	−39.2	Cation−π + Electrostatic	Arg163, Tyr185	Stable interaction via aromatic and charged residue engagement
7-Hydroxymitragynine	*Mitragyna speciosa*	AXL Kinase	−38.5	−36.9	H-bond + Hydrophobic	Asp70, Phe36	Balanced interaction with strong conformational stability

Table 7: RMSD-Based Structural Consistency of Representative Ligand–Receptor Complexes

Ligand	Source	Target Receptor	RMSD (Å)	Binding Affinity Trend	Structural Interpretation
21-Hydroxydammar-24-en-3-one	*Garuga pinnata*	TGF-βRII (3DKC)	0.586	Very strong	Highly stable binding pose with favorable deep-pocket accommodation
Garuganin-V1_Et	*Garuga pinnata*	TGF-βRII	1.284	Strong	Flexible scaffold supports consistent pocket alignment
Garuganin-V1_Me	*Garuga pinnata*	TGF-βRII	1.567	Strong	Compact structure maintains stable binding orientation
7-Acetoxymitragynine	*Mitragyna speciosa*	AXL kinase (5U6B)	1.890	Very strong	Stable conformation with effective electrostatic anchoring
Mitraphylline-26	*Mitragyna speciosa*	TGF-βRII	1.245	Strong	Rigid scaffold ensures limited structural deviation
7-Hydroxymitragynine	*Mitragyna speciosa*	AXL kinase	1.303	Strong	Low structural deviation indicates stable docking geometry

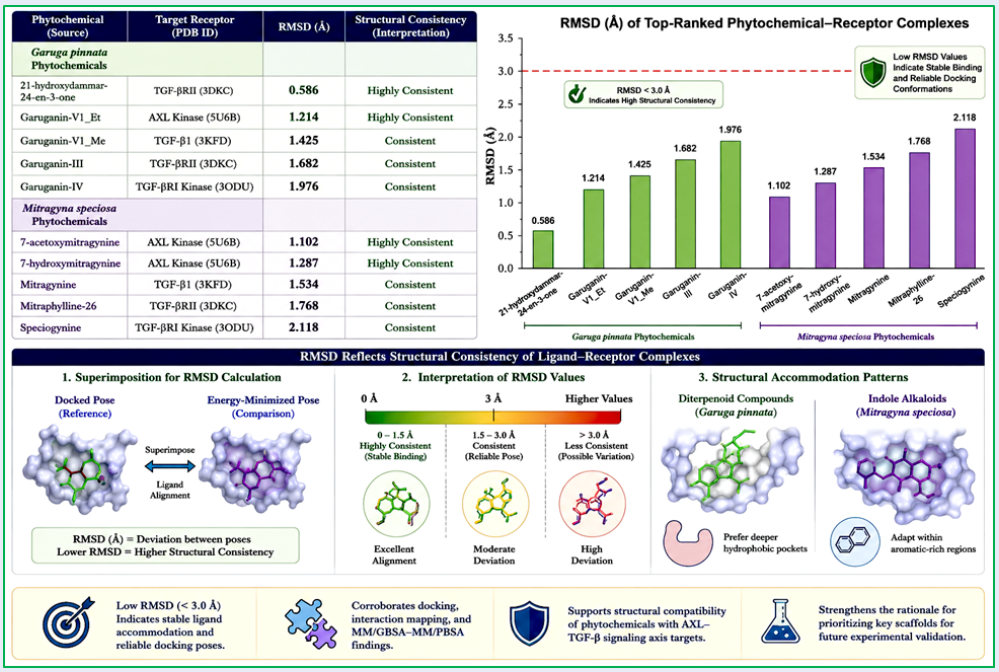

Figure 4: Comparative post-docking receptor–ligand interaction profiles of selected *Garuga pinnata* and *Mitragyna speciosa* phytochemicals across the AXL–TGF-β signaling axis. Representative three-dimensional binding conformations and two-dimensional interaction diagrams of the highest-ranked phytochemicals docked with AXL kinase (PDB ID: 5U6B), TGF-β1 (3KFD), TGF-β receptor II (3DKC), and TGF-β receptor I kinase (3ODU) are shown, illustrating binding orientations, key interacting residues, and intermolecular interactions within the predicted active sites.

tions across multiple metastasis-associated targets. The convergence of docking affinities, residue-level interaction mapping, and MM/GBSA–MM/PBSA energy estimates indicated that these compounds were capable of engaging conserved functional regions within both AXL kinase and TGF-β receptor systems.

Notably, the complementary binding behavior observed between diterpenoid and indole alkaloid scaffolds suggested a scaffold-dependent multi-target interaction pattern, enabling effective accommodation within diverse receptor pocket environments. Within the constraints of a static computational framework, these findings supported the prioritization of selected phytochemicals as candidate multi-target ligands with potential relevance to the modulation of metastatic signaling pathways.

DISCUSSION

The present study integrated molecular docking, interaction mapping, binding free energy estimation, and structural consistency analysis to examine how phytochemicals from *Garuga pinnata* and *Mitragyna speciosa* interacted with metastasis-associated receptors, including AXL kinase and the TGF-β signaling system. Taken together, the results indicated that selected diterpenoid and indole alkaloid scaffolds adopted favorable binding orientations, formed coherent interaction networks, and exhibited energetically consistent conformations within receptor binding pockets, supporting their ability to engage conserved functional regions across multiple targets[32].

A key novelty of this work lay in the simultaneous multi-target evaluation of ethnomedicinal phytochemicals against the AXL–TGF-β signaling axis, a synergistic pathway critically implicated in epithelial–mesenchymal transition (EMT) and metastatic progression[33,34]. Unlike conventional single-target *in silico* studies, this investigation adopted an integrated framework to assess cross-target binding behavior, revealing a scaffold-dependent interaction pattern. Diterpenoid compounds preferentially occupied deeper catalytic clefts dominated by hydrophobic interactions, whereas indole alkaloids aligned along

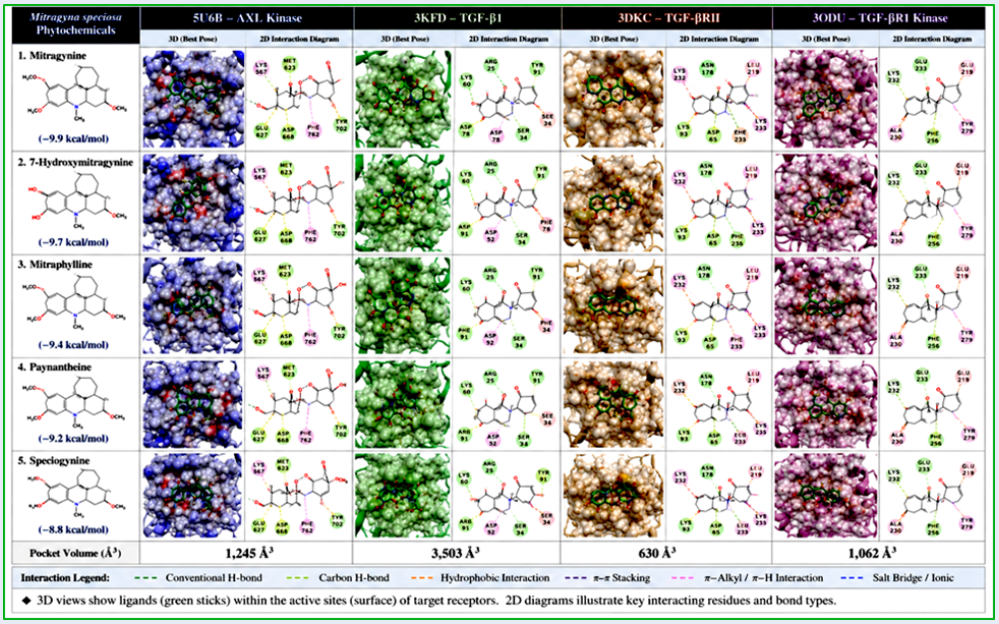

Figure 5: Comparative post-docking receptor–ligand interaction profiles of selected *Mitragyna speciosa* phytochemicals across the AXL–TGF-β signaling axis. Representative three-dimensional binding conformations and two-dimensional interaction diagrams of the highest-ranked *Mitragyna speciosa* phytochemicals docked with AXL kinase (PDB ID: 5U6B), TGF-β1 (3KFD), TGF-β receptor II (3DKC), and TGF-β receptor I kinase (3ODU) are shown, illustrating ligand-binding orientations, key interacting amino acid residues, and intermolecular interactions within the predicted active sites.

aromatic and amphipathic regions, enabling π-mediated and electrostatic stabilization. This complementary binding behavior highlighted a structurally driven adaptability that may be advantageous for multi-target modulation[35,36].

At the residue level, conserved acidic and basic amino acids (e.g., Asp, Glu, Arg, Lys) contributed to directional hydrogen bonding and electrostatic stabilization, while aromatic residues facilitated π–π and cation–π interactions[37]. These interaction features were consistent with the observed docking affinities and MM/GBSA–MM/PBSA energy trends, particularly for top-ranking ligands such as 21-hydroxydammar-24-en-3-one and 7-acetoxymitragynine, which demonstrated stable and well-accommodated binding geometries across multiple receptors. The integration of structural topology, interaction mapping, and energetic profiling further represented a methodological advancement for prioritizing multi-target candidates derived from ethnopharmacological sources.

The RMSD-based assessment supported the consistency of docked conformations, with low deviation values indicating stable binding poses within predicted pockets. However, these findings were derived from energy-minimized static structures and did not account for time-dependent conformational flexibility, solvent dynamics, or entropic contributions. Accordingly, the reported stability reflected structural consistency rather than dynamic stability, aligning with the scope of a hypothesis-generating computational study.

From a biological perspective, the ability of these phytochemicals to interact with both AXL kinase and TGF-β receptors suggested potential relevance in modulating EMT, cellular migration, and metastatic progression. The observed multi-target interaction pattern aligned with emerging therapeutic strategies aimed at overcoming pathway redundancy in complex diseases such as cancer[38,39]. Nevertheless, these implications remained predictive and exploratory, pending experimental validation.

Several limitations should be acknowledged. The reliance on static docking and post-docking energy calculations provided relative binding estimates but did not fully capture the dynamic behavior of ligand–receptor complexes. The absence of molecular dynamics simulations limited insight into long-term conformational stability, and no ex-

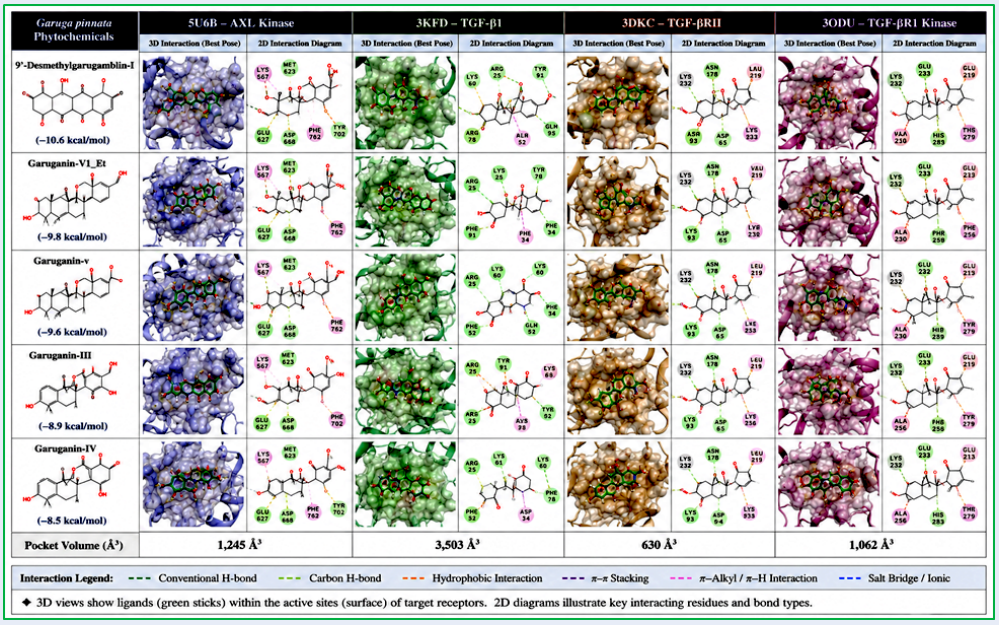

Figure 6: Structural consistency and conformational stability of the highest-ranked phytochemical–receptor complexes. RMSD-based comparison demonstrates the structural reliability of docking-derived binding conformations for selected *Garuga pinnata* phytochemicals interacting with AXL kinase (5U6B), TGF-β1 (3KFD), TGF-β receptor II (3DKC), and TGF-β receptor I kinase (3ODU). Low RMSD values indicate minimal conformational deviation and favorable ligand accommodation within receptor binding pockets, corroborating the docking, interaction mapping, and MM/GBSA–MM/PBSA analyses.

perimental validation was conducted to confirm biological activity[40,41]. Future work should therefore incorporate trajectory-based molecular dynamics simulations to evaluate kinetic stability and solvent effects, followed by experimental validation, including biochemical binding assays and cell-based functional studies targeting EMT and metastatic markers. Additionally, structure-guided optimization and pharmacokinetic evaluation would be essential to translate these findings into viable therapeutic candidates[42]. Overall, this study presented a novel integration of ethnomedicinal knowledge with multi-target structure-based computational screening, offering a rational framework for identifying phytochemical scaffolds with potential relevance in metastasis-related pathways. The identification of scaffold-dependent, multi-receptor binding behavior provided new insight into the design of multi-target therapeutic strategies and supported further investigation into phytochemical-based drug discovery.

CONCLUSION

This study highlights the potential of *Garuga pinnata* and *Mitragyna speciosa* as valuable sources of natural compounds that may target the AXL–TGF-β signaling axis, a key regulator of epithelial–mesenchymal transition (EMT), tumor invasion, and metastasis. By combining molecular docking, MM/GBSA–MM/PBSA binding free-energy calculations, and RMSD-based structural assessment, we identified several phytochemicals that consistently showed favorable binding affinities, stable interaction patterns, and reliable structural conformations across multiple metastasis-associated receptors. Interestingly, the two plant species exhibited complementary binding characteristics. Diterpenoids from *Garuga pinnata* interacted effectively within hydrophobic receptor pockets, whereas indole alkaloids from *Mitragyna speciosa* adapted well to aromatic-rich binding environments. Despite these structural differences, both groups of compounds formed stable hydrogen bonds, hydrophobic contacts, and π-mediated interactions, suggesting their potential to modulate multiple components of the metastatic signaling network. Although these findings are based on computational analyses, the strong agreement among docking, binding energy, and structural consistency results provides confidence in the predicted ligand–receptor interactions. Future molecular dynamics simulations and

experimental validation will be essential to confirm their biological activity. Overall, this study demonstrates how integrating traditional medicinal knowledge with modern computational approaches can accelerate the identification of promising natural-product leads for the development of future anti-metastatic therapies.

ABBREVIATIONS

AXL: AXL receptor tyrosine kinase
EMT: Epithelial–mesenchymal transition
MM/GBSA: Molecular Mechanics/Generalized Born Surface Area
MM/PBSA: Molecular Mechanics/Poisson–Boltzmann Surface Area
RMSD: Root Mean Square Deviation
TGF-β: Transforming Growth Factor-beta

ACKNOWLEDGMENTS

The authors gratefully acknowledge the collaborative support of the Department of Forest, Government of Madhya Pradesh, and Sri Aurobindo Medical College and Post Graduate Institute (SAIMS Hospitals), Sanwer Road, Indore, Madhya Pradesh, India, under Sri Aurobindo University, for providing the facilities, institutional support, and research environment necessary for this study. The authors also express their sincere gratitude to Dr. Vinod Bhandari, Founder Chairman, Sri Aurobindo Group of Institutes (SAIMS), Indore, for his visionary leadership, continued encouragement, and unwavering commitment to promoting excellence in research and innovation.

AUTHOR'S CONTRIBUTIONS

Mohammad Nadeem Khan conceptualized and designed the study, performed computational analysis, interpreted the data, prepared figures and tables, and drafted the manuscript. Mahak Bhandari assisted in data compilation, formatting, and visualization. Ashok Kumar contributed to critical revision of the manuscript and overall scientific validation. Praveen Chandra Dubey assisted in data interpretation and methodological evaluation. Sanjay Vyas contributed to study supervision, scientific review, and manuscript refinement. Shushil Upadhayay contributed to literature analysis and manuscript editing. All authors reviewed, approved, and agreed to the final version of the manuscript.

FUNDING

The authors declare that no external funding was received for this study.

AVAILABILITY OF DATA AND MATERIALS

All data generated or analyzed during this study are included in this published article.

ETHICS APPROVAL AND CONSENT TO PARTICIPATE

Not applicable. This study involved computational analysis using publicly available databases and did not involve human participants or animal experimentation.

CONSENT FOR PUBLICATION

Not applicable.

DECLARATION OF GENERATIVE AI AND AI-ASSISTED TECHNOLOGIES IN THE WRITING PROCESS

AI-assisted language refinement tools were used solely for improving grammar, language clarity, formatting, and manuscript organization. All scientific interpretations, computational analyses, and final content validation were performed exclusively by the authors.

COMPETING INTERESTS

The authors declare that they have no competing interests.

REFERENCES

1. Goyette MA, Côté JF. AXL receptor tyrosine kinase as a promising therapeutic target directing multiple aspects of cancer progression and metastasis. Cancers (Basel). 2022 Jan;14(3):466. PMID: 35158733. Available from: https://doi.org/10.3390/cancers14030466.
2. Myers SH, Brunton VG, Unciti-Broceta A. AXL inhibitors in cancer: a medicinal chemistry perspective. J Med Chem. 2016 Apr;59(8):3593–3608. PMID: 26555154. Available from: https://doi.org/10.1021/acs.jmedchem.5b01273.
3. Batlle E, Massagué J. Transforming growth factor-β signaling in immunity and cancer. Immunity. 2019 Apr;50(4):924–940. PMID: 30995507. Available from: https://doi.org/10.1016/j.immuni.2019.03.024.
4. Dongre A, Weinberg RA. New insights into the mechanisms of epithelial-mesenchymal transition and implications for cancer. Nat Rev Mol Cell Biol. 2019 Feb;20(2):69–84. PMID: 30459476. Available from: https://doi.org/10.1038/s41580-018-0080-4.
5. Liao J, Chen R, Lin B, Deng R, Liang Y, Zeng J, et al. Crosstalk between the TGF-β and cell adhesion signaling pathways in cancer. Int J Med Sci. 2024 May;21(7):1307–1320. PMID: 38818471. Available from: https://doi.org/10.7150/ijms.96274.
6. Victoir B, Croix C, Gouilleux F, Prié G. Targeted therapeutic strategies for the treatment of cancer. Cancers (Basel). 2024 Jan;16(2):461. PMID: 38275901. Available from: https://doi.org/10.3390/cancers16020461.
7. Ganesh K, Massagué J. Targeting metastatic cancer. Nat Med. 2021 Jan;27(1):34–44. PMID: 33442008. Available from: https://doi.org/10.1038/s41591-020-01195-4.

8. Wu S, Liao M, Li M, Sun M, Xi N, Zeng Y. Structure-based discovery of potent inhibitors of Axl: design, synthesis, and biological evaluation. RSC Med Chem. 2022 Jul;13(10):1246–1264. PMID: 36325401. Available from: https://doi.org/10.1039/D2MD00153E.
9. Katz LH, Li Y, Chen JS, Muñoz NM, Majumdar A, Chen J, et al. Targeting TGF-β signaling in cancer. Expert Opin Ther Targets. 2013 Jul;17(7):743–760. PMID: 23651053. Available from: https://doi.org/10.1517/14728222.2013.782287.
10. Wu F, Li J, Jang C, Wang J, Xiong J. The role of Axl in drug resistance and epithelial-to-mesenchymal transition of non-small cell lung carcinoma. Int J Clin Exp Pathol. 2014 Sep;7(10):6653–6661. PMID: 25400744.
11. Sang YB, Kim JH, Kim CG, Hong MH, Kim HR, Cho BC, et al. The development of AXL inhibitors in lung cancer: recent progress and challenges. Front Oncol. 2022 Mar;12:811247. PMID: 35311091. Available from: https://doi.org/10.3389/fonc.2022.811247.
12. Choudhari AS, Mandave PC, Deshpande M, Ranjekar P, Prakash O. Phytochemicals in cancer treatment: from preclinical studies to clinical practice. Front Pharmacol. 2020 Jan;10:1614. PMID: 32116665. Available from: https://doi.org/10.3389/fphar.2019.01614.
13. Singla RK, Bishayee A. Anticancer drug discovery based on natural products: from computational approaches to clinical studies. Cancers (Basel). 2025 Jul;17(15):2507. PMID: 40805204. Available from: https://doi.org/10.3390/cancers17152507.
14. Uddin M, Sarker MS, Mamun MJ, Quader JM, Alim MA, Meem JN. Medicinal attributes of Garuga pinnata Roxb.: a systematic exploration of its analgesic, antidiarrheal, hypoglycemic, and cytotoxic activities. Asian J Res Bot. 2025;8(2):537–554. Available from: https://doi.org/10.9734/ajrib/2025/v8i2285.
15. Begum T, Arzmi MH, Khatib A, Uddin AB, Aisyah Abdullah M, Rullah K, et al. A review on *Mitragyna speciosa* (Rubiaceae) as a prominent medicinal plant based on ethnobotany, phytochemistry and pharmacological activities. Nat Prod Res. 2025 Mar;39(6):1636–1652. PMID: 38923960. Available from: https://doi.org/10.1080/14786419.2024.2371564.
16. Mesta S, Kumar J, Elayaperumal S, Meenakumari H. Advances in Ethnomedicine and Phytomedicine. Singapore: Springer; 2024. Available from: https://doi.org/10.1007/978-981-97-3405-4_21.
17. Vivek-Ananth RP, Mohanraj K, Sahoo AK, Samal A. IMPPAT 2.0: an enhanced and expanded phytochemical atlas of Indian medicinal plants. ACS Omega. 2023 Feb;8(9):8827–8845. PMID: 36910986. Available from: https://doi.org/10.1021/acsomega.3c00156.
18. O'Boyle NM, Banck M, James CA, Morley C, Vandermeersch T, Hutchison GR. Open Babel: an open chemical toolbox. J Cheminform. 2011 Oct;3(1):33. PMID: 21982300. Available from: https://doi.org/10.1186/1758-2946-3-33.
19. Daina A, Zoete V. Application of the SwissDrugDesign online resources in virtual screening. Int J Mol Sci. 2019 Sep;20(18):4612. PMID: 31540350. Available from: https://doi.org/10.3390/ijms20184612.
20. Burley SK, Berman HM, Duarte JM, Feng Z, Flatt JW, Hudson BP, et al. Protein Data Bank: a comprehensive review of 3D structure holdings and worldwide utilization by researchers, educators, and students. Biomolecules. 2022 Oct;12(10):1425. PMID: 36291635. Available from: https://doi.org/10.3390/biom12101425.
21. Burley SK, Berman HM, Bhikadiya C, Bi C, Chen L, Di Costanzo L, et al. RCSB Protein Data Bank: biological macromolecular structures enabling research and education in fundamental biology, biomedicine, biotechnology and energy. Nucleic Acids Res. 2019 Jan;47(D1):D464–D474. PMID: 30357411. Available from: https://doi.org/10.1093/nar/gky1004.
22. Ye B, Tian W, Wang B, Liang J. CASTpFold: computed atlas of surface topography of the universe of protein folds. Nucleic Acids Res. 2024 Jul;52(W1):W194–W199. PMID: 38783102. Available from: https://doi.org/10.1093/nar/gkae415.
23. Liu Y, Yang X, Gan J, Chen S, Xiao ZX, Cao Y. CB-Dock2: improved protein-ligand blind docking by integrating cavity detection, docking and homologous template fitting. Nucleic Acids Res. 2022 Jul;50(W1):W159–W164. PMID: 35609983. Available from: https://doi.org/10.1093/nar/gkac394.
24. Jiang D, Du H, Zhao H, Deng Y, Wu Z, Wang J, et al. Assessing the performance of MM/PBSA and MM/GBSA methods. 10. Prediction reliability of binding affinities and binding poses for RNA-ligand complexes. Phys Chem Chem Phys. 2024 Mar;26(13):10323–10335. PMID: 38501198. Available from: https://doi.org/10.1039/D3CP04366E.
25. King E, Aitchison E, Li H, Luo R. Recent developments in free energy calculations for drug discovery. Front Mol Biosci. 2021 Aug;8:712085. PMID: 34458321. Available from: https://doi.org/10.3389/fmolb.2021.712085.
26. Hollingsworth SA, Dror RO. Molecular dynamics simulation for all. Neuron. 2018 Sep;99(6):1129–1143. PMID: 30236283. Available from: https://doi.org/10.1016/j.neuron.2018.08.011.
27. Filipe HA, Loura LM. Molecular dynamics simulations: advances and applications. Molecules. 2022 Mar;27(7):2105. PMID: 35408504. Available from: https://doi.org/10.3390/molecules27072105.
28. Wang Z, Sun H, Shen C, Hu X, Gao J, Li D, et al. Combined strategies in structure-based virtual screening. Phys Chem Chem Phys. 2020 Feb;22(6):3149–3159. PMID: 31995074. Available from: https://doi.org/10.1039/C9CP06303J.
29. Talele TT, Khedkar SA, Rigby AC. Successful applications of computer aided drug discovery: moving drugs from concept to the clinic. Curr Top Med Chem. 2010;10(1):127–141. PMID: 19929824. Available from: https://doi.org/10.2174/156802610790232251.
30. Huang M, Lu JJ, Ding J. Natural products in cancer therapy: past, present and future. Nat Prod Bioprospect. 2021 Feb;11(1):5–13. PMID: 33389713. Available from: https://doi.org/10.1007/s13659-020-00293-7.
31. Najafi M, Mortezaee K, Majidpoor J. Cancer stem cell (CSC) resistance drivers. Life Sci. 2019 Oct;234:116781. PMID: 31430455. Available from: https://doi.org/10.1016/j.lfs.2019.116781.
32. Youssef KK, Nieto MA. Epithelial-mesenchymal transition in tissue repair and degeneration. Nat Rev Mol Cell Biol. 2024 Sep;25(9):720–739. PMID: 38684869. Available from: https://doi.org/10.1038/s41580-024-00733-z.
33. Vijayan Y, Sandhu JS, Harikumar KB. Modulatory role of phytochemicals/natural products in cancer immunotherapy. Curr Med Chem. 2024;31(32):5165–5177. PMID: 38549529. Available from: https://doi.org/10.2174/0109298673274796240116105555.
34. Zhang S, Liu K, Liu Y, Hu X, Gu X. The role and application of bioinformatics techniques and tools in drug discovery. Front Pharmacol. 2025 Feb;16:1547131. PMID: 40017606. Available from: https://doi.org/10.3389/fphar.2025.1547131.
35. Macalino SJ, Gosu V, Hong S, Choi S. Role of computer-aided drug design in modern drug discovery. Arch Pharm Res. 2015 Sep;38(9):1686–1701. PMID: 26208641. Available from: https://doi.org/10.1007/s12272-015-0640-5.
36. Salem MM, Mohamed TM. Targeting cancer signaling pathways and their therapeutic strategies. Discov Oncol. 2026 Mar;17(1):548. PMID: 41855011. Available from: https://doi.org/10.1007/s12672-026-04708-8.
37. Sambi M, Bagheri L, Szewczuk MR. Current challenges in cancer immunotherapy: multimodal approaches to improve efficacy and patient response rates. J Oncol. 2019 Feb;2019:4508794. PMID: 30941175. Available from: https://doi.org/10.1155/2019/4508794.
38. B-Rao C, Subramanian J, Sharma SD. Managing protein flexibility in docking and its applications. Drug Discov Today. 2009 Apr;14(7-8):394–400. PMID: 19185058. Available from: https://doi.org/10.1016/j.drudis.2009.01.003.
39. Weth FR, Hoggarth GB, Weth AF, Paterson E, White MP, Tan ST, et al. Unlocking hidden potential: advancements, approaches, and obstacles in repurposing drugs for cancer therapy. Br J Cancer. 2024 Mar;130(5):703–715. PMID: 38012383.

Available from: https://doi.org/10.1038/s41416-023-02502-9.

40. Atanasov AG, Zotchev SB, Dirsch VM, Supuran CT. International Natural Product Sciences Taskforce. Natural products in drug discovery: advances and opportunities. Nat Rev Drug Discov. 2021 Mar;20(3):200–216. PMID: 33510482. Available from: https://doi.org/10.1038/s41573-020-00114-z.
41. Bharti R, Mujwar S, Singh P, Singh TG, Khatri N. A computational approach for screening of phytochemicals from Oxalis corniculata as promising anti-cancer candidates. J King Saud Univ Sci. 2024;36(9):103383. Available from: https://doi.org/10.1016/j.jksus.2024.103383.
42. Baldi S, Long N, Ma S, Liu L, Al-Danakh A, Yang Q, et al. Advancements in Protein Kinase Inhibitors: From Discovery to Clinical Applications. Research (Wash D C). 2025 Jun;8:0747. PMC12180671. PMID: 40547482. Available from: https://doi.org/10.34133/research.0747.